

Radioactive beams and inverse kinematics: probing the quantal texture of the nuclear vacuum

F. Barranco¹, G. Potel², E. Vigezzi³, and R. A. Broglia^{4,5}

¹ Departamento de Física Aplicada III, Escuela Superior de Ingenieros, Universidad de Sevilla, Camino de los Descubrimientos, 41092 Sevilla, Spain

² National Superconducting Cyclotron Laboratory, Michigan State University, East Lansing, MI 48824, USA

³ INFN Sezione di Milano, via Celoria 16, I-20133 Milano, Italy

⁴ The Niels Bohr Institute, University of Copenhagen, DK-2100 Copenhagen, Denmark

⁵ Dipartimento di Fisica, Università degli Studi di Milano, Via Celoria 16, I-20133 Milano, Italy

the date of receipt and acceptance should be inserted later

Abstract. The properties of the quantum electrodynamic (QED) vacuum in general, and of the nuclear vacuum (ground) state in particular are determined by virtual processes implying the excitation of a photon and of an electron–positron pair in the first case and of, for example, the excitation of a collective quadrupole surface vibration and a particle–hole pair in the nuclear case. Signals of these processes can be detected in the laboratory in terms of what can be considered a nuclear analogue of Hawking radiation. An analogy which extends to other physical processes involving QED vacuum fluctuations like the Lamb shift, pair creation by γ -rays, van der Waals forces and the Casimir effect, to the extent that one concentrates on the eventual outcome resulting by forcing a virtual process to become real, and not on the role of the black hole role in defining the event horizon. In the nuclear case, the role of this event is taken over at a microscopic, fully quantum mechanical level, by nuclear probes (reactions) acting on a virtual particle of the zero point fluctuation (ZPF) of the nuclear vacuum in a similar irreversible, no–return, fashion as the event horizon does, letting the other particle, entangled with the first one, escape to infinity, and eventually be detected. With this proviso in mind one can posit that the reactions $^1\text{H}(^{11}\text{Be}, ^{10}\text{Be}(2^+; 3.37 \text{ MeV}))^2\text{H}$ and $^1\text{H}(^{11}\text{Li}, ^9\text{Li}(1/2^-; 2.69 \text{ MeV}))^3\text{H}$ together with the associated γ -decay processes indicate a possible nuclear analogy of Hawking radiation.

PACS. 2 1.60.Jz, 23.40.-s, 26.30.-k

1 Introduction

At the basis of quantum mechanics one finds Heisenberg’s indeterminacy relations, Born–Jordan commutation rules, Pauli principle, Born probability interpretation of Schrödinger wave function and Dirac transformation theory. All these elements find natural imagery in Feynman diagrams, and call for the existence of a vacuum state, whose structure is determined by virtual processes. These processes, which do not conserve energy, modulate the quantum vacuum through the transient presence of fermionic particles and antiparticles and of bosonic quanta. In the case of the electromagnetic vacuum permeating space, these are virtual off-shell electron–positron pairs and photons (Fig. 1(I)(a)). If some of these elements are modified through the action of an external field which provides in the process energy, angular and linear momentum, etc., the remaining particles can become on-shell and thus the vacuum radiates. Reaching the detector, this radiation provides information on the virtual states, and thus on the texture of the vacuum, let alone on the event triggering the radiation.

Let us build the case one step at a time, and start considering pair creation in the laboratory by a photon (left wavy line and vertex, Fig. 2(a)). Because the created pair has invariant finite mass, while the photon has zero mass, a second interaction is necessary. In Fig. 2(a), it is provided by a second photon (lower right wavy line) and associated vertex, reflecting the action of a massive charge Z (cross labeled Z) needed for momentum conservation. It is of notice that in all vertices one finds three particles. This is in keeping with the fact that in QED the interaction acting at each vertex is bilinear in fermions (electrons, positrons) and linear in bosons (photons) (see App. A). Within this context, the process associated with the vertex to the left in Fig. 2(a) plays the same role as the lower vertex of Fig. 1(a)(I). Returning to Fig. 2(a), if one allows the electron to annihilate with the positron (closing the loop) and absorb the photon (left wavy line), one obtains the Feynman diagram of Fig. 1(a)(I), as the presence of the massive charge Z and associated photon is not needed.

By collapsing the two vertices and the massive charge

of the QED Feynman diagram of Fig. 2 (a) into a single vertex assumed to result from the action of the curved gravitational space associated with a black hole (cylinder), one can adapt 2 (a) to Hawking's heuristic diagram (Fig. 2 (b); see [1,2]). We return to this point below, but before let us consider the possibility to subject the QED vacuum to a supercritical atomic nucleus of effective charge $Z > Z_{crit} \approx 180$, resulting from a quasimolecular state transiently formed in a heavy ion collision. Under such conditions the QED vacuum state is expected to become charged, positrons being emitted at the same time. The vacuum rearranges in such a way so as to minimise the effect of the applied "external" field. That is, the vacuum acts as a screening medium. A schematic representation of such a process is given in Fig. 2(c). The heavy grey lines provide a schematic representation of the two ions at the distance of closest approach, of the order of 16 fm. The transient, quasimolecular state of charge $Z = Z_1 + Z_2 > Z_{crit}$ leads to a multi photon process of pair creation [3,4,5].

As in the black hole case, the $Z > Z_{crit}$ situation shows a preferred distance (radius) for the occurrence of the phenomenon leading to particle emission. In the simplest black hole description it is the Schwarzschild radius, while in the heavy ion collision leading to Z_{crit} it is that of the radius of the 1s orbital with $\epsilon_{s_{1/2}} < -2m_e c^2$ of the quasimolecular system.

In a similar way in which Hawking's approach [1] is based on a classical (relativistic) gravitational picture, the calculation of the heavy ion collision eventually leading to the $Z_1 + Z_2 = Z_{cr}$ is described in a time-dependent semiclassical approximation up to the distance of closest approach. But from that point on, the pair production and associated radiation process is carried out quantum mechanically, as testified by the QED Feynman diagram (c) of Fig. 2. Within this context it is in principle thinkable to follow a similar approach in dealing with Hawking radiation and instead of (b) Fig. 2, use a diagram similar to (c). It is of notice that while the Z_{crit} heavy ion reaction positron production phenomenon did not lead, in spite of much experimental effort, to a conclusive answer [6], a similar "shake off" phenomenon of the QED vacuum was observed in the process $\omega + n\omega_0 \rightarrow e^+e^-$ for $n \geq 4$ laser photons of wavelength 527 nm colliding with a photon energy of 29 GeV [7]. Within this context see also [8, 9] and references therein.

In the above scenario nothing precludes the possibility of the presence of both photons and gravitons in the corresponding Feynman diagrams. In fact this seems to be the most likely situation, as shown in [10] in connection with photon emission from a charged particle falling into a black hole, described within the framework of QED and found to be of Hawking type, although some nontrivial differences with the "classical" result were found.

QED vacuum fluctuations play also a central role in the Lamb shift [11,12,13,14,15], as seen from Figs. 1 (II)(b)-(d) and Fig. 3 (C) (see also [16]). The corresponding self-energy processes depend on the atomic orbital occupied by the electron. In the case of hydrogen it leads to a split-

ting between the $^2P_{1/2}$ and $^2S_{1/2}$ orbital of 1058 MHz. Within this context, we mention that Hawking refers to the Lamb shift as a phenomenon which provides confirmation of virtual fluctuations of QED [2]. As mentioned above, this phenomenon implies processes involving photons, aside from electrons and positrons (Figs. 1 (II) (b)-(d)) and Fig. 3). The fact that Hawking states that quantum mechanics implies that the *whole* of space (and not only that close to the event horizon of black holes) is filled with pairs of "virtual" particles and antiparticles that are constantly materialising in pairs must imply that he views the process displayed in Fig. 1 (a) (right, i.e. with a photon) equivalent to that shown on the left, where the photon is represented by the associated electromagnetic field.

Let us now briefly mention the Casimir effect [17,18, 19,20], originally intended to provide a quantum mechanical description of the van der Waals force [21,22,23,24,25, 26] acting between two non-polar molecules, taking into account retardation effects. The results obtained correspond to the long-wavelength limit of the Feynman diagram shown in Fig. 4 (d), and connected with vacuum ZPF. In other words, while it is true that the Casimir energy can be expressed in terms of Feynman diagrams with external legs [20], this does not mean that they are not a direct consequence of QED vacuum zero point fluctuations (within this context see Figs. 1 (II)(b) and (d) and 4 (a)-4 (d)). The Casimir effect is referred to, if not by name, quite explicitly on p.202 of [1], in connection with the statement that the black hole being an excited state of the gravitational field can decay quantum mechanically and that because of quantal fluctuations, energy should be able to tunnel out of the corresponding potential well, a particle creation analogous to that caused by a deep potential well in flat space (confinement of two infinite walls) [24]. It is of notice that a detailed determination of the Casimir effect requires surface plasmons to be considered [27]. Within the nuclear connection it is closely connected with induced nuclear interaction, in particular induced pairing interaction [28,29,30].

2 Hawking radiation

After the above has been stated, we can use Fig. 1 I (b) in what follows. We start with the left hand side representation of electromagnetic quantum fluctuations (Fig. 1 I (a)), for then use the QED description (right hand side Feynman diagram).

At the zero point fluctuation (ZPF) domain centered around r_0 , all particles can, in principle, become real (on shell). Adopting a simple Newtonian description, this can happen in the case of the electron-positron pair, provided

$$(m_e c^2 + T_{e^-} + (U_G)_{e^- - bh}) + (m_e c^2 + T_{e^+} + (U_G)_{e^+ - bh}) = 0, \quad (1)$$

where $(U_G)_{i-bh}$ is the gravitational interaction energy between the black hole (bh , of mass m_{bh}) and the electron and positron (e^- , e^+ , m_e). The quantities T_{e^-} and T_{e^+} are the kinetic energies associated with these fermions. The

functions $U_G(r)$ vanish at $r = \infty$, the remaining quantities being all positive. Thus, both particles cannot be emitted together as HR . But if one of them falls behind the event horizon characterised by the Schwarzschild radius ($r_s = 2Gm_{bh}/c^2$), and the associated gravitational energy $(U_G)_{i-bh}$ is sufficiently negative, the on-shell condition can eventually be fulfilled and HR emitted.

Assuming the electron escapes to infinity ($(U_G)_{e^- - bh} = 0$) with kinetic energy T_{e^-} , the trapped (infalling) positron-black hole gravitational interaction provides the negative energy necessary to fulfill global energy conservation. Because the subsystem ($bh + e^+$) has less energy than the original bh , one can posit that the bh has lost mass which has been emitted as an electron (HR).

Let us now consider the case in which the pair materialises through an elementary QED vacuum fluctuation (Fig. 1 (I)(b) right hand side diagram). The above equation should then include the photon energy and associated gravitational interaction with the bh field,

$$(h\nu_0 + (U_G)_{ph-bh}) + (m_e c^2 + T_{e^-} + (U_G)_{e^- - bh}) + (m_e c^2 + T_{e^+} + (U_G)_{e^+ - bh}) = 0, \quad (2)$$

where $h\nu_0$ is the photon energy while $m_{ph} = h\nu/c^2$ is the photon mass entering $(U_G)_{ph-bh}$. Being three the particles present in the vacuum ZPF (Fig. 1 I (a) right), a variety of escape combinations are possible. It is sensible to think that a bh radiates as a black body. Thus, all possible particles combinations as well as final-state interactions are expected to be present, similarly to what happens in QED pair creation by a supercritical Coulomb field (Fig. 2 (c)). Because not only gravitons can induce pair production, but also photons in presence of the bh , the situation resembles that of the "classical" result for the Casimir force per unit area between two parallel plates separated by a distance d ($F_C = -\hbar c \pi^2 / (240 \times d^4)$) [23]. In fact, this expression is only valid in the limit $\alpha \rightarrow 0$ of the fine structure constant, and assuming perfect conductivity. As mentioned above, the QED expression of the Van der Waals force between two metallic plates depends on the corresponding surface plasma, let alone on α [20, 27].

In the case in which the photon escapes as HR (Fig. 1 (I)(b)), it will eventually be observed that the original emission frequency undergoes a strong gravitational red shift. Being emitted near the event horizon, the asymptotic ($r = \infty$) frequency is

$$h\nu_\infty = h\nu_0 \left(1 - \frac{r_s}{r_0}\right)^{1/2} = h\nu_0 + (U_G(r_0))_{ph-bh} + \dots \quad (3)$$

Regarding the process in which the photon associated with the vacuum ZPF falls behind the horizon, $E_{HR} = 2m_e c^2 + T_{e^-} + T_{e^+}$ (Fig. 1 (I)(c)). Assuming electron-positron pair annihilation takes place (in presence of the massive object which ensures linear momentum conservation), may lead to photon production of frequency $\nu' \geq 2m_e c^2/h$.

Predicted more than forty years ago [1], Hawking radiation through which black holes lose energy and mass,

eventually evaporating (primordial black holes), still awaits experimental confirmation. In fact, it is difficult if not impossible to observe Hawking radiation from a real black hole, (see however [31]) and analogue black-hole experiments are being studied in search for alternative examples of it (cf. [32, 33] and refs. therein).

3 Nuclear Field Theory: structure and reactions of exotic nuclei

Quantum electrodynamics (QED) in Feynman formulation provides a detailed description of the electromagnetic vacuum, paradigm of the quantum vacuum [34]. Nuclear field theory (NFT), tailored after Feynman's graphical version of QED, supplemented by renormalization, allows for a quantal description of nuclear structure in general and of the nuclear vacuum in particular [35, 36, 37, 38].

In this description particles (p) and holes (h), namely nucleons moving above and missing from the Fermi sea respectively, play the role of electrons and positrons. They are to be calculated as solutions of the Hartree-Fock mean field. Collective vibrations, play the role of photons. The strength of the particle-vibration coupling vertices play the role of the fine structure constant. Such vertices are to be summed up to infinite order to calculate the vibrations which, at variance to the photon, are composite modes. A further difference is that the "nuclear photons" come in a number of species, namely of ph -type (e.g. surface vibrations) of, pp -type (pairing vibrations), as well as a variety of spin, isospin, etc. quantum numbers.

Worked out in the seventies in connection with nuclear structure NFT has been further developed to systematically deal with spontaneously broken symmetries and associated phase transitions and Goldstone modes [39], and generalized to deal, on equal footing, with structure and reactions [40, 41]. Making use of renormalization techniques, convergence in non-perturbative situations can be ensured [38]. NFT has been applied to deal with a wide variety of phenomena throughout the mass table, providing an overall account of the experimental findings at the 10% level [42, 43], and predictions which tested, were found in accordance with observations at a similar level of accuracy [44, 45, 46].

Because of its graphical rules, NFT allows to make parallels and find unexpected connections with many-body theories of condensed matter and cluster physics [47, 48], let alone QED. In particular, in connection with analogues to the Lamb shift in the systematic probing of the nuclear quantum vacuum (ground state) (see Fig. 3 and e.g. [42]). This is the reason why it appears natural to elaborate on a possible parallel between nuclear phenomena (structure and reactions), and Hawking radiation. Connection extended to the Casimir effect triggered by the remark found on p. 202 of [1], namely: "This particle creation is directly analogous to that caused by a deep potential well in flat space-time". In other words, pair production of QED vacuum under stress (constrain).

In this connection we also note that the realistic description of the Casimir effect involves the consideration of

the fluctuations of the QED vacuum (exchange of virtual photons). Generalizing these phenomena to the dynamical Casimir effect (conducting plates in relative acceleration) the connection with HR through Einstein's equivalence principle emerges in a natural fashion [49,50]. Given the parallel existing between NFT and QED, replacing the moving plates by the colliding nuclei in a nuclear reaction, the nuclear analogue of HR seems permissible.

Reactions using exotic radioactive nuclei in inverse kinematics and active cell targets setups have brought the study of the nuclear structure and reactions to unexpected heights and technical refinements. This is mainly a consequence of the efforts made to achieve a complete description of the nuclei under study, reflected in the use of a wide variety of probes leading to Coulomb excitation and inelastic scattering and associated γ -decay, as well as inducing one- and two-nucleon transfer reactions. This is particularly so in the probing of nuclei lying at the edge of matter stability as is the case of neutron drip line systems. Paradigmatic examples of such developments are studies carried out at TRIUMPH [51], Saclay and GANIL [52] and RIKEN [53], which have provided, among other things, detailed information on the vacuum state of exotic nuclei. The reason for concentrating our attention on these nuclei is because, being weakly bound and close to the neutron drip line, they display very large fluctuations.

The zero point fluctuations associated with ^{11}Be and ^{11}Li cores (see Fig. 1 (II)(a) as well as boxed inset), self energy contribution of the parity inverted (Fig. 3) ground state $1/2^+$ of ^{11}Be (Fig. 1 (II) (d)), see also Fig. 5 (I) (a)) and of the induced pairing correlation of the halo neutrons of ^{11}Li (Figs. 6 (b) where also a 1^- vibration is to be considered in this last case), contribute approximately 6.3% and 4.7% of the corresponding binding energies, respectively (Table 1). A major fraction of the associated ZPF mass defect in these nuclei is contributed by processes which involve the quadrupole modes: 86% in the case of ^{11}Be and 74% in that of ^{11}Li (for details of the general framework see e.g. [54] and refs. therein).

Direct experimental insight into the mechanism at the basis of the above results in particular, and of the structure properties of the two halo nuclei in question can be obtained through one- and two-nucleon processes, namely [55] $^1\text{H}(^{11}\text{Be}, ^{10}\text{Be}((2^+; 3.368 \text{ MeV}))^2\text{H}$ and [45] $^1\text{H}(^{11}\text{Li}, ^9\text{Li}(1/2^-; 2.69 \text{ MeV}))^3\text{H}$.

The mass relations, which parallel (2) are in these cases (see Fig. 5 (I)(b),(d)–(f) in relation to the first reaction and Fig. 6 (c) in connection with the second one),

$$M(ZX_f)c^2 = M(ZX_i)c^2 - h\nu_{2+} + ((\Delta m)c^2 + \Delta T), \quad (4)$$

with

$$\Delta m = \begin{cases} (m_p - m_d) & [((ZX_i, ZX_f) \equiv (^{11}_4\text{Be}, ^{10}_4\text{Be}))], \\ (m_p - m_t) & [((ZX_i, ZX_f) \equiv (^{11}_3\text{Li}, ^9_3\text{Li}))], \end{cases} \quad (5)$$

and

$$\Delta T = \begin{cases} (T(^{11}\text{Be}) - T(^{10}\text{Be}) - T_d, & [(Z = 4)], \\ (T(^{11}\text{Li}) - T(^9\text{Li}) - T_t, & [(Z = 3)], \end{cases} \quad (6)$$

where p , d , and t label proton, deuteron and triton respectively. The term inside parentheses in the left hand side of (3) takes into account the kinetic energy of the projectile inducing the nuclear reaction and of the resulting outgoing particles, the other term being associated with the reaction Q -value. Although the outcome of the γ -coincidence experiment (related to the $h\nu_{2+}$ term in (4)) can be taken for granted, its actual measurement in processes based on inverse kinematics like the ones under consideration, is technically quite trying and has not yet been measured. Be as it may, the fact that the calculated absolute transfer differential cross sections provide an overall account of the experimental findings [42,46] gives direct insight into the soundness, the (renormalised) NFT picture of the nuclear vacuum state, has (see Fig. 5 (I)(c) and lower inset of Fig. 6).

Let us now return to Fig. 1 (II). The bare properties of an odd nucleon moving around the core (Fig. 1 (II)(b)) get modified though Pauli principle corrections (Fig. 1 (II)(c)) and through the associated dressing process resulting from its time ordering (Fig. 1 (II)(d)). Within the scenario of quantum electrodynamics (QED) where Feynman diagrams were developed, and in keeping with the symmetry existing between positron and electron phase spaces, \mathbf{N} -like and self-energy-like [34] processes (Figs. 1 (II)(c) and (d)) are operative on equal footing. Observation of any of the associated virtual processes dressing the electron by interrupting it through the action of an external field (e.g. Fig. 1 (III)(b)), carries similar information concerning both contributions II(c) and (d). Because of spatial quantisation, finite nuclei display an asymmetry between occupied and empty states (particles and holes). As a consequence process (c) of Fig. 1 (II) may be allowed and not process (d), or viceversa. This is particularly true for light nuclei, for example ^{11}Be [42].

In the core of ^{11}Be , namely $^{10}_4\text{Be}_6$, six neutrons occupy the $1s_{1/2}$ and $1p_{3/2}$ levels (Fig. 3). The dominant ZPF is of quadrupole type, the main neutron component being associated with the $((p_{1/2}, p_{3/2}^{-1}) \otimes 2^+)_{0+}$ ZPF (Fig. 5(II)(a)). Because $\epsilon_{p_{1/2}} - \epsilon_{p_{3/2}} \approx 3.38 \text{ MeV}$ and $\hbar\omega_{2+} = 3.368 \text{ MeV}$, the largest amplitude of the wavefunction of the quadrupole mode is associated with the neutron particle-hole excitation $(p_{1/2}, p_{3/2}^{-1})_{2+}$. The repulsion due to Pauli principle correction (Fig. 3 inset (A)) is $\approx 2.86 \text{ MeV}$. The clothing of the $2s_{1/2}$ bare level by the quadrupole mode (Fig. 3 inset (B)) makes it heavier, lowering its energy by about 0.5 MeV (570 keV). The result of the two processes mentioned above is parity inversion, and the appearance of the $N = 6$ new magic number together with the melting away of the $N = 8$ standard one. In a similar way in which the Lamb shift (Fig. 3, inset C) provides a measure of the fluctuations of the QED vacuum (see [56], p. 451), parity inversion measures ZPF of the nuclear vacuum (ground) state. In this last case further information can be obtained as compared with the atomic case, through particle transfer reactions.

Let us elaborate on this point. Interpreting the arrowed lines of Fig. 1 (III)(a) as an electron and a positron, the wavy curve as a photon and the external field (cross +

dashed line) as the event horizon of a black hole (see Fig. 1 (I)(b)) one has a Feynman representation of Hawking radiation. A nuclear analogue of such radiation, to the extent that one considers only the wavy line and the detector click, is provided by graph (b) of Fig. 1 (III), if one interprets the arrowed line as a nucleon, the wavy line as a nuclear vibration and the external field (open square+dashed line) as a irreversible and nucleon pickup reaction intervening the self-energy process shown in Fig. 1 (II)(d) at a time t fulfilling $t_0 < t < t_1$. A concrete example of the above parlance is provided by the no return event corresponding to the one neutron pickup reaction of the single-halo valence nucleon of ^{11}Be , leading to the population of the low-lying quadrupole, first excited (vibrational) state of the core ^{10}Be , as shown in Figs. 5 (I)(b),(e) and (c) (see also Fig. 5 (II) in relation with the spontaneous γ -decay of the 2^+ state, in coincidence with the reaction process).

Light nuclei at the drip line provide another paradigmatic example of parity inversion and of a nuclear analogue, again in the sense of a virtual process becoming real through the irreversible action of an external field. The nucleus is ^{11}Li , the no return event in question the process $^1\text{H}(^{11}\text{Li}, ^9\text{Li}(1/2^-; 2.69 \text{ MeV}))^3\text{H}$ (Fig. 6 (c)). The $|^{11}\text{Li}(\text{gs})\rangle$ can be viewed as a two-neutron halo pair addition mode (double arrowed line) and a proton moving in the $p_{3/2}$ orbital which acts as a spectator. In Figs. 6 (a) and (b), virtual processes associated with self-energy and induced pairing interaction (vertex corrections) are shown (for details see ref. [44]). Acting with an external two-nucleon pickup field at a time t such that $t_0 < t < t_1$, leads to the population of the $|^{11}\text{Li}(1/2^-; 2.69 \text{ MeV})\rangle$ first excited state with an absolute differential cross section (Fig. 6, lower part) accounting for the experimental findings (see ref. [45]).

4 Entanglement and correlations

The characteristic trait of quantum mechanics is the fact that when two systems, of which one knows the states through their respective wavefunctions enter into temporary physical interaction, and when after a time of mutual influence the systems separate again, then they can no longer be described in the same way as before, as they have become entangled. After reestablishing one wavefunction by observation, the other one can be inferred simultaneously [59]. With the proviso that detector sensitivity is adequate to cope with background noise, let alone set up to pick up the specific signal of the phenomenon under study. A macroscopic manifestation of quantum entanglement is provided by superconductivity in bulk metals at low temperature, and by Josephson current through an unbiased junction. The Josephson effect provides a macroscopic manifestation of quantum entanglement. But to detect the supercurrent circulating through an unbiased

junction between two weakly coupled superconductors it is necessary to go from standard 100Ω junctions easy to operate with, to 1Ω ones, let alone eliminate the earth magnetic field, as well as to carry out quantitative investigations to distinguish the effect from tiny superconducting shorts [60,61].

Within this context, arguably, is it possible to set in the proper perspective the failure to detect the QED vacuum instability through collisions between very heavy ions. This is in keeping with the complexity of calculating absolute cross sections in such cases [40], let alone analyze experiments associated with highly excited, massive nuclei which eventually can convert their many-body energy into pairs (e^-, e^+) [6]. At variance, in the case of direct reactions, in particular those under discussion ((p, d) , (p, t)), carried out at moderate bombarding energies ($3 \text{ MeV}/A$), only few channels and elementary modes of excitation are open and active respectively. Furthermore one, in these cases, knows how to calculate absolute cross sections which reproduce the experimental findings within a 10% error.

Within this context it is of notice that the probabilities of populating the final state $1/2^-$ in the reaction $^{11}\text{Li}(p, t)^9\text{Li}(1/2^-; 2.691 \text{ MeV})$ through channels alternative to the direct, one-step ones, are considerably less important. They lead to cross sections which are three orders of magnitude smaller than experimentally observed (see Fig. 6 (d), and Table I of ref. [46]). A similar situation is expected in the case of the population of the first 2^+ excited state of ^{11}Be in the reaction $^{11}\text{Be}(p, d)^{10}\text{Be}(2^+; 3.368 \text{ MeV})$ [55]. Concerning entanglement of the escaping Hawking particle (detected γ -ray) with its partner(s) swallowed in the black hole (picked up in the no-return reaction process), the nuclear examples under discussion are amenable to a technically trying, but straightforward control, known as coincidence experiments. Namely, to accept events in which the photon ($\hbar\nu_{2^+}=3.368 \text{ MeV}$) and the deuteron (Fig 5 (e)) or the photon ($\hbar\nu_{2^+}=2.691 \text{ MeV}$) and the triton (Fig. 6 (c)) are recorded gating the corresponding detectors at the energy $\hbar\nu_{2^+}$ and at that resulting from (4) respectively. Entanglement which extends over the physical dimensions of modern RIB laboratory detector setups.

An alternative, simpler experiment, which carries equal *bona fide* quantum mechanical entanglement information but is arguably less technically demanding is the following. Identify only the nature of the outgoing particle, or set up a γ -detector array to record a single line of frequency ν_{2^+} and intensity $I_\gamma \pm a$. The quantity I_γ is related to the absolute transfer cross section and a to the associated experimental error. In this way one eliminates any possible contributions from other channels but the direct one (see e.g. Fig. 6 (d)).

From a quantum mechanical point of view, once the click in the γ -detector has disentangled the outgoing (2_1^+ vibration \rightarrow (γ -decay), see Fig. 6 (d)) particle wavefunction Ψ_γ from that of the two halo neutrons Ψ_{2n} , one knows also this one, and the no return event (although most likely the $2n$ system long before has ended up as heat in the accelerator shielding). Namely, the falling of $2n$ into the

¹ Spontaneous γ -decay is a direct consequence of the ZPF of the nuclear vacuum (through its proton component) due to the presence of the ZPF of the electromagnetic field.

	$BE/A(\text{keV})$	$BE_{ZPF}(\text{keV})$	$BE(\text{keV})$	$BE_{ZPF}/BE (\times 10^{-2})$
^{11}Be	5952.54 ± 22	4110	65477.94	6.3
^{11}Li	4155.38 ± 6	2150	45709.18	4.7

Table 1. Binding energy BE and binding energy per nucleon BE/A (both in keV) (see [57] and Suppl. material of this reference) associated with the nuclei ^{11}Be and ^{11}Li . The ZPF contribution to the binding energy of these two nuclei (see ref. [54] for details of the general framework) arises from dipole, quadrupole and octupole (p, h) vibrations and from monopole pair vibrational modes (see also [58]).

no-return triton potential leading to $\Psi_t = f(\Psi_p, \Psi_{2n})$ (Ψ_p describing the proton beam), and thus to its $(2n)$ ultimate fate. Viceversa, observing Ψ_t but not measuring neither the energy nor the momentum of the triton, provides complete information on Ψ_γ , and of the presence of a γ -ray of frequency ν_{2+} and intensity I_γ . Whether it reaches the detector or ends up contributing to the (local) background radiation or detector shielding heat, is a question of detector budget.

But the possibilities within the scenario of entanglement and correlation in nuclear structure and reactions are richer than anticipated above. In fact, by changing the bombarding energy of the proton one expects a resonant behaviour when the de Broglie wavelength matches a value related to the wavelength of $h\nu_{2+}$ in each of the reactions considered (self energy processes Figs. 5 (a) and (d), and Fig. 6 (a)) but also that of the dipole mode in the second one (vertex correction, induced pairing, Fig. 6 (b)) which essentially provides all of the small but finite ($S_{2n} = 380$ keV) energy, binding the two halo neutrons to the core ^9Li . By making the proton beam oscillate between the differential cross sections resonant behaviour bombarding energies associated with $h\nu_{2+}$ and $h\nu_{1-}$, one would mimic a kind of self-amplifying Hawking radiation. Technical difficulties likely restricts this to remain an only *gedanken eksperiment*.

Nonetheless, in the nuclear case, there are further degrees of entanglements. At the level of nuclear structure, in keeping with the fact that the bosonic elementary modes of excitation are not elementary but composite two-quasiparticle-like collective excitations. At the level of nuclear reactions in which case two-nucleon transfer is completely dominated by successive transfer, due to the fact that the correlation energy of Cooper pairs is much smaller than the Fermi energy ($\approx 10^{-2}$ in the case of ^{11}Li), and that the correlation length between members of the pair is larger than nuclear dimensions.

Let us elaborate on these points, using as examples $|^{11}\text{Li}(\text{gs})\rangle$, $|^{11}\text{Li}(1^-; 750 \text{ keV})\rangle$ and $|^9\text{Li}(2^+; 3.368 \text{ MeV})\rangle$ and the reaction $^{11}\text{Li}(p, t)^9\text{Li}(1^-; 2.691 \text{ MeV})$. In all these states it is assumed that the $p_{3/2}(\pi)$ odd proton acts as a spectator and thus we do not write it for simplicity. We start with $|^{11}\text{Li}(\text{gs})\rangle$, namely the two neutron halo pairing correlated system. Making use of the microscopic random phase approximation (RPA) and of the quasiparticle RPA (QRPA) description of $|^9\text{Li}(2^+; 3.368 \text{ MeV})\rangle$ and of $|^{11}\text{Li}(1^-; 750 \text{ keV})\rangle$ respectively, one can calculate the self-energy contributions and the induced pairing interaction (vertex corrections) shown in Figs. 6 (a) and (b),

using also the v_{14} Argonne potential as the bare $NN^{-1}S_0$ bare pairing interaction. Propagating these processes to infinite order by solving a Dyson-like equation, one obtains an accurate description of the experimental findings (for details see [38] and [46]).

In Fig. 7 (a) and (b) we display the resulting spatial correlations of the two neutrons in $|^{11}\text{Li}(\text{gs})\rangle$ and compare it with the pure configuration $1p_{1/2}^2(0)$, an important component of the ground state of ^{11}Li . Similar results are shown in connection with the 2^+ of ^9Li and the 1^- of ^{11}Li (Figs. 7 (c) and (d) and (e), (f)). The importance of the correlation is apparent.

Let us concentrate now on entanglement regarding the two-nucleon transfer process. As seen in Fig. 6 (d), the transfer of one nucleon at a time, that is successive transfer, constitutes the main contribution to the transfer process. From the particle-particle correlation displayed in Fig. 7 (a) and (b), and the fact that the two neutrons in the triton are close by (~ 2 fm) one would have expected simultaneous transfer to be the main component. Now, the probability of neutron tunneling decreases exponentially with the square root of the mass. Because pairing correlations have a coherence length larger than nuclear dimensions, it is thus profitable that one nucleon tunnels at a time. Said it differently, to calculate the probability P_2 of a two-particle transfer process of a pair of correlated nucleons, one has to add the phased single-particle tunneling probability amplitudes, before taking the absolute square value, that is

$$P_2 = \left| \frac{e^{i\phi_1}\sqrt{P_1} + e^{-i\phi_2}\sqrt{P_1}}{2} \right|^2 = \frac{P_1}{2}(1 + \cos(\phi_1 + \phi_2)), \quad (7)$$

and thus $P_2 \approx P_1$ ($\phi_1 + \phi_2 \approx 0$), a result which parallels that found by Anderson [60] in connection with the Josephson effect. Typical examples of $P_2 \approx P_1$ in the nuclear case are provided by [45]

$d\sigma(^9\text{Li}(d, p)^{10}\text{Li}(1/2^-))/d\Omega|_{\theta_{max}} \approx 0.8 \text{ mb/sr}$, as compared to [62] $d\sigma(^{11}\text{Li}(p, t)^9\text{Li}(1/2^-))/d\Omega|_{\theta_{max}} \approx 1 \text{ mb/sr}$, [63] $^{10}\text{Be}(t, p)^{12}\text{Be}(\text{gs})$ ($\sigma = 1.9 \pm 0.5 \text{ mb}$, $4.4^\circ \leq \theta_{cm} \leq 54.4^\circ$) as compared to [64] $^{10}\text{Be}(d, p)^{11}\text{Be}(1/2^+)$ ($\sigma = 2.4 \pm 0.013 \text{ mb}$, $5^\circ \leq \theta_{cm} \leq 39^\circ$) in the case of light nuclei around closed ($N = 6$) shell, and [65] $^{120}\text{Sn}(p, t)^{118}\text{Sn}(\text{gs})$ ($\sigma = 3.024 \pm 0.907 \text{ mb}$, $5^\circ \leq \theta_{cm} \leq 40^\circ$) as compared to [66] $^{120}\text{Sn}(d, p)^{121}\text{Sn}(7/2^+)$ ($\sigma = 5.2 \pm 0.6 \text{ mb}$, $2^\circ \leq \theta_{cm} \leq 58^\circ$).

Let us now discuss the correlation between particles and holes (ph) associated with the two quasiparticle (pp, ph, hh)

states 2_1^+ and 1^- , and at the basis of the phenomena of core polarization responsible for the dressing of particles (self energy) and the renormalization of the ph and (pp, hh) interactions (vertex and pairing renormalization).

As seen from Figs. 7 (c), (d) and (e), (f), the (ph) become closer together when correlated by the quadrupole and the dipole residual interaction, respectively. Emitted and reabsorbed by single nucleons (Fig. 3, Fig. 5 I (a), (d), Fig. 6 (a)) they give rise to the quasiparticle degrees of freedom carrying effective masses (energies) and spectroscopic amplitudes (single-particle content), as experimentally observed (see e.g. [42,43] and refs. therein). Exchanged between nucleons they renormalise the bare nucleon–nucleon interaction, in particular the 1S_0 pairing interaction (see e.g. [28,29] and refs. therein), effects which can be treated in nuclear field theory also to infinite order of perturbation if needed, in particular in the case of superfluid nuclei, but also of halo nuclei like ^{11}Li . Ground state correlations of ph collective modes and associated renormalization effects provide non negligible contributions to the binding energies (see Figs. 5 (II) (a)–(c), Table 1 and e.g. [54] and refs. therein). They are also essential in reproducing the experimental value of the electromagnetic transition probabilities. In fact, dressing the collective vibrations, e.g. the collective quadrupole mode of ^{120}Sn , leads to conspicuous increase in the $B(E2)$ -value associated with the decay into the ground state [67], in overall agreement with the experimental findings.

Clearly, this can hardly be connected with whether particles and holes are close in space, as the wavelength of γ -rays of 1–2 MeV are orders of magnitude larger than nuclear dimensions. In fact, it is related to the fact that the components of the wavefunctions of collective states are phase-correlated, as is the case in pp correlated states (pairing vibrations like ^{11}Li (gs))) and associated two-particle, mainly successive, transfer.

A summary of correlation and entanglement simultaneously operative at the level of structure and reaction discussed above, is shown in Fig. 8, for the case of the process $A+2 X + p \rightarrow A X(J^\pi; E_x) + t$ (e.g. $^{11}\text{Li} + p \rightarrow ^9\text{Li}(1/2^-; 2.69 \text{ MeV}) + t$). The small (grey) ellipses focus on the particle–particle (neutron–neutron) correlations. That is, a structure property which is calculated for the systems $(A+2)$ and t ($\equiv ^3\text{H}$) in isolation. The corresponding wavefunctions describe the effect of both (pp) -correlation (weak), as well as that of the external single-particle field (strong). The large ellipse focus on the (pp) entanglement taking place in the transfer process, dominated by the mechanism of successive transfer. The outgoing triton and γ -ray (resulting from the $E2$ -decay of the quadrupole mode of the core A (^9Li)) are entangled and bring the specific information regarding the correlation existing between the fermionic partners of the Cooper pair, closely connected with the transfer formfactor. The (p, t) is an irreversible, no-return process providing the energy, momentum both linear and angular for the γ ray to become on shell. The variety of processes are treated fully quantum mechanically and on equal footing, within the full single-particle space, described by both bound and continuum states.

5 Conclusions

The vacuum state of a quantal system contains, through zero point fluctuations, virtual information concerning the particles (elementary modes of excitation in the case of a many-body system) building the system, and their interactions (interweaving). To bring this information to the detector, one needs to intervene the virtual states, in a no-return fashion, with external fields which share the properties one wants to observe. In the nuclear case, one-particle transfer to learn about single-particle motion, Cooper pair transfer to get information concerning the mechanisms by which gauge invariance can be violated (Cooper pair binding). Doing so in the case of light halo nuclei we have learned that, in a similar way in which the Lamb shift provided in the H-atom a definitive answer to Rabi's question of whether the polarisation of a QED vacuum could be measured, parity inversion in nuclei provides a definitive answer of the central role collective vibrations play both in the dressing processes of valence nucleons, as well as in the induced pairing interaction acting among them, as testified by the Hawking-like radiation observed in the $^1\text{H}(^{11}\text{Be}, ^{10}\text{Be}(2^+)) ^2\text{H}$ and $^1\text{H}(^{11}\text{Li}, ^9\text{Li}(1/2^-)) ^3\text{H}$ reaction processes, respectively. To be able to recover information contained in the vacuum associated with the field theoretical description of the nuclear structure (s), NFT had to be extended to be able to describe also reaction processes (r) to the same level of accuracy, and making use of the same language [38]. In particular, treating on equal footing non-orthogonality and non-locality of the elementary modes of excitation as well as simultaneous, successive and non-orthogonality (non-local-)contributions to Cooper pair tunnelling. Within this context, one can refer to the simultaneous renormalisation of single-particle energies and transfer form factors as a further consequence of the above $(s+r)$ unification requirement.

Say it differently, we have critically assessed experimental information shedding light on one- and two-neutron halo nuclei ^{11}Be [55] and ^{11}Li [45] respectively, discuss the texture of the associated nuclear vacuum and point to possible nuclear parallels to Hawking radiation in the sense of the abstract. It is of notice that in spite of much effort, a theory of quantum gravity which unifies general relativity and quantum mechanics does not yet exist. The prediction of Hawking radiation results from a combination of these two theories. In the nuclear case, a unified quantal description of structure and reactions (which play the role of the irreversible, no-return event), taking into account nonlocality and retardation both concerning correlations and transfer mechanisms and involving also electromagnetic decay, is available within the framework of renormalised NFT [38].

It is our hope that the subjects discussed in the present paper, presenting a new view of nuclear dynamics in connection with black hole Hawking radiation can act as intellectual stimulus concerning a full quantum treatment of the phenomena involved. From our part we consider this the first step of a major challenge which we plan to follow up in future publications.

6 Acknowledgment

R.A.B. is grateful to L. Mandelli for discussions as well as to C. Pethick for suggestions. F.B. and E.V. acknowledge funding from the European Union Horizon 2020 research and innovation program, under Grant Agreement No. 654002. F.B. acknowledges funding from the Spanish Ministerio de Economía under Grant Agreement FIS2014-53448-C2-1-P.

A Feynman rules for calculating the S-matrix in QED

One considers electrons, positrons and photons. A possible gauge- and Lorentz-invariant Lagrangian for QED is

$$\mathcal{L} = -\frac{1}{4}F_{\mu\nu}F^{\mu\nu} - \bar{\Psi}(\gamma^\mu[\partial_\mu + ieA_\mu] + m)\Psi \quad (8)$$

where

$$F_{\mu\nu}(x) = \partial_\mu A_\nu(x) - \partial_\nu A_\mu(x), \quad (9)$$

m being the electron mass, γ^μ Dirac matrices and one sums over indices like μ and ν which appear twice, one upstairs and the other downstairs. The electric current four-vector is

$$J^\mu = \frac{\partial \mathcal{L}}{\partial A_\mu} = -ie\bar{\Psi}\gamma^\mu\Psi. \quad (10)$$

The interaction is

$$V(t) = ie \int d^3x (\bar{\Psi}(\mathbf{x}, t)\gamma^\mu\Psi(\mathbf{x}, t))a_\mu(\mathbf{x}, t) + V_{coul}, \quad (11)$$

where electrons are created and annihilated by fields $\bar{\Psi}$ and Ψ , while the photon is created and annihilated by fields a_μ , the instantaneous Coulomb field $V_{coul}(t)$ just serving to cancel the part of the photon propagator that is non-covariant and local in time, and

$$\mathbf{A}(\mathbf{x}) = \sum_{\lambda=\pm} \int \widetilde{dk} \left[\epsilon_\lambda^*(\mathbf{k})a_\lambda(\mathbf{k})e^{ikx} + \epsilon_\lambda(\mathbf{k})a_\lambda^\dagger(\mathbf{k})e^{-ikx} \right], \quad (12)$$

where $k^0 = \omega = |\mathbf{k}|$, $\widetilde{dk} = d\mathbf{k}/2(\pi)^3 2\omega$ and ϵ_+ and ϵ_- are polarization vectors. Let us now remind some of the Feynman rules for calculating the connected part of the S -matrix of quantum electrodynamics. In particular the first one: (i) draw all Feynman diagrams with up to some number of vertices. The diagrams consist of electron lines carrying arrows, with the lines joined at the vertices, a each of which there is one incoming and one outgoing electron line and one photon line. Examples of diagrams containing two vertices are provided by lowest-order Compton scattering and electron-positron scattering (Fig. 9 (a) and (b), respectively).

Another two-vertex diagram is obtained by joining in graph (a) the photon lines and the electron lines, in this last case going backwards in time, and the 1' - 2' and 1 - 2

electron line in (b). The resulting diagram (e) describes the lowest order vacuum fluctuation.

In drawing these diagrams one should exclude disconnected diagrams, that is, diagrams in which any $V(t)$ operator or any initial or final particle is not connected to every other one by a sequence of particle creations and annihilations. Examples are provided by diagrams (c), (d) and (f) of Fig. 9.

If one views the disconnected electron line in (f) as describing the electron of an hydrogen atom, virtual fluctuations can affect the energy levels, in particular that of the $2s_{1/2}, 2p_{1/2}$ levels predicted by Dirac equation to have the same energy. This is because the electron in the zero point fluctuation (ZPF) of the vacuum may partially occupy the same state occupied by the electron of the hydrogen atom.

The exchange of the virtual and the disconnected electron lines correct for Pauli principle violation, leading to the connected two-vertex diagram (g) (identical to (h)) and, by time ordering, to diagram (i). The energy denominators, associated with these diagrams, difference of the initial and of the intermediate state energy are $Den_{(h)} = -(E_N + E_M + \omega)$ and $Den_{(i)} = [E_N - (E_M + \omega)]$ respectively. In these expressions E_N is the energy of the electron in the initial state, the energy of the intermediate state being either the sum of the energy E_M of an electron and a photon of energy ω (Fig. 9 (i)), or else a positron of energy E_M , a photon of energy ω , plus $2E_N$, sum of the energy of both initial and final electrons (Fig. 9 (h)).

The resulting value of the difference between the summed contributions (h) + (i) associated with the $2s_{1/2}$ and $2p_{1/2}$ states of the hydrogen atom from relativistic calculations leads to $[\delta E]_{2s} - [\delta E]_{2p_{1/2}} = 1052.19$ MHz [16] (see also [13, 14, 15], and [12]) as compared to the experimental value 1057.845(9) MHz [68], the value reported by the first experiment and (non-relativistic) theoretical calculations being 1000 MHz [11] and 1040 MHz respectively [12]. As exemplified by the Feynman diagrams shown in Fig. 9, by construction and as a direct consequence of the interaction (A.4) which is bilinear in electron fields and linear in photon fields, associated with each vertex there are two electron (positron) lines and one photon line. In particular in the case of the process shown in Fig. 9 (e), namely a two vertex Feynman diagram describing the zero point fluctuations of the QED vacuum.

As recounted by Pais [56, 69], Lamb provided a quantitative answer, both experimentally and theoretically [14, 11] to the question of Rabi of whether the polarisation of the vacuum could be measured. According to quantum mechanics, intervening a virtual process as a result of a conservation law or a physical principle (external field), in the present case the exclusion principle, one can probe the structure of the associated off-the-energy-shell process. Within this context and of the Lamb shift phenomenon, the need of a three lines, two electrons (positrons) and one photon, virtual process in connection with QED vacuum fluctuations is apparent.

It could be argued that an electron-positron vacuum

virtual excitation can be a valid QED Feynman diagram interpreting the vertices as the result of the action of a Coulomb field. As stated in connection with Eq. (A.5), the violation of Lorentz invariance by the instantaneous Coulomb interaction, is cancelled by another apparent violation of Lorentz invariance connected with the fact that the photon fields a_μ are not four vectors, and therefore have a non-covariant propagator. The important point is that the photon propagator is taken effectively as a covariant quantity

$$\Delta_{\mu\nu}^{eff}(x-y) = (2\pi)^{-4} \int d^4q \frac{\eta_{\mu\nu}}{q^2 - i\epsilon} e^{iq(x-y)} \quad (13)$$

with the Coulomb interaction dropped. From a practical point of view, the main issue is that in the momentum space Feynman rules, the contribution of an internal photon line is given by

$$\frac{-i}{(2\pi)^4} \frac{\eta_{\mu\nu}}{q^2 - i\epsilon}, \quad (14)$$

and the Coulomb interaction dropped, as reflected by (A.5) (for details see [16]).

References

1. S. W. Hawking. Particle creation by black holes. *Commun. Math. Phys.*, 43:199, 1975.
2. S. W. Hawking. The quantum mechanics of black holes. *Sci. Am.*, 236:34, 1977.
3. Berndt Müller, Heinrich Peitz, Johann Rafelski, and Walter Greiner. Solution of the Dirac Equation for Strong External Fields. *Phys. Rev. Lett.*, 28:1235, 1972.
4. J. Rafelski, B. Müller, and W. Greiner. The charged vacuum in over-critical fields. *Nuclear Physics B*, 68:585, 1974.
5. Gerhard Soff, Joachim Reinhardt, Berndt Müller, and Walter Greiner. Shakeoff of the vacuum polarization in quasi-molecular collisions of very heavy ions. *Phys. Rev. Lett.*, 38:592, 1977.
6. J. Rafelski, B. Müller, J. Reinhardt, and W. Greiner. Probing QED vacuum with heavy ions. *arXiv:1604.08690v1*, 2016.
7. D. L. Burke, R. C. Field, G. Horton-Smith, J. E. Spencer, D. Walz, S. C. Berridge, W. M. Bugg, K. Shmakov, A. W. Weidemann, C. Bula, K. T. McDonald, E. J. Prebys, C. Bamber, S. J. Boege, T. Koffas, T. Kotseroglou, A. C. Melissinos, D. D. Meyerhofer, D. A. Reis, and W. Ragg. Positron production in multiphoton light-by-light scattering. *Phys. Rev. Lett.*, 79:1626, 1997.
8. Cesim K. Dumlu and Gerald V. Dunne. Stokes Phenomenon and Schwinger Vacuum Pair Production in Time-Dependent Laser Pulses. *Phys. Rev. Lett.*, 104:250402, 2010.
9. J. Q. Yu, H. Y. Lu, T. Takahashi, R. H. Hu, Z. Gong, W. J. Ma, Y. S. Huang, C. E. Chen, and X. Q. Yan. Creation of electron-positron pairs in photon-photon collisions driven by 10-pw laser pulses. *Phys. Rev. Lett.*, 122:014802, 2019.
10. R. Parentani. Hawking radiation from feynman diagrams. *Phys. Rev. D*, 61:027501, 1999.
11. Willis E. Lamb and Robert C. Retherford. Fine structure of the hydrogen atom by a microwave method. *Phys. Rev.*, 72:241, 1947.
12. H. A. Bethe. The electromagnetic shift of energy levels. *Phys. Rev.*, 72:339, 1947.
13. Theodore A. Welton. Some observable effects of the quantum-mechanical fluctuations of the electromagnetic field. *Phys. Rev.*, 74:1157, 1948.
14. Norman M. Kroll and Willis E. Lamb. On the self-energy of a bound electron. *Phys. Rev.*, 75:388, 1949.
15. J. B. French and V. F. Weisskopf. The electromagnetic shift of energy levels. *Phys. Rev.*, 75:1240, 1949.
16. S. Weinberg. *The Quantum Theory of Fields*, volume 1. Cambridge University Press, Cambridge, 1996.
17. H. B. G. Casimir. Hydrophobicity at Small and Large Length Scales. *Proc. K. Ned. Akad. Wet.*, 60:793, 1948.
18. H. B. G. Casimir. On the interaction between two perfectly conducting plates. *Proc. K. Ned. Akad. Wet. B*, 51:793, 1948.
19. H. B. G. Casimir and D. Polder. The influence of retardation on the london-van der waals forces. *Phys. Rev.*, 73:360, 1948.
20. R. L. Jaffe. Casimir effect and the quantum vacuum. *Phys. Rev. D*, 72:021301, 2005.
21. F. London. Zur Theorie der Systematik der Molekularkräfte. *Z. f. Physik*, 63:245, 1930.
22. F. London. The general theory of molecular forces, *Trans. Faraday Soc.*, 33:8, 1937.
23. E. M. Lifschitz. The theory of molecular attractive forces. *J. Exp. Theor. Phys. USSR*, 29:94, 1955.
24. J. B. Bjorken and S. D. Drell. *Relativistic quantum mechanics*. Mc Graw-Hill, New York, 1998.
25. J. N. Israelachvili. *Intermolecular and surface forces*. Academic Press, New York, 1985.
26. L. Pauling and Wilson Jr. E. B. *Quantum Mechanics*. Dover, New York, 1963.
27. F. Intravaia. The role of surface plasmons in the casimir effect. *arXiv:0706.1184v2*, 2007.
28. F. Barranco, R. A. Broglia, G. Gori, E. Vigezzi, P. F. Bortignon, and J. Terasaki. Surface vibrations and the pairing interaction in nuclei. *Phys. Rev. Lett.*, 83:2147, 1999.
29. J. Terasaki, F. Barranco, R. A. Broglia, E. Vigezzi, and P. F. Bortignon. Solution of the Dyson equation for nucleons in the superfluid phase. *European Physical Journal A*, 697:127, 2002.
30. Brink, D. and R. A. Broglia. *Nuclear Superfluidity*. Cambridge University Press, Cambridge, 2005.
31. D. An, K.A. Meissner, and R. Penrose. Apparent evidence for hawking points in the CMB sky. *arXiv:1808.01740v1*, 2018.
32. J. Steinhauer. Observation of quantum hawking radiation and its entanglement in an analogue black hole. *Nature Physics*, 12:959, 2016.
33. D. Castelvecchi. Artificial black hole creates its own version of hawking radiation. *Nature News*, 536:258, 2016.
34. S.S. Schweber. *QED*. Princeton University Press, Princeton, New Jersey, 1994.
35. D. R. Bès, G. G. Dussel, R. A. Broglia, R. Liotta, and B. R. Mottelson. Nuclear field theory as a method of treating the problem of overcompleteness in descriptions involving elementary modes of both quasi-particles and collective type. *Phys. Lett. B*, 52:253, 1974.

36. Bortignon, P. F., R. A. Broglia, D. R. Bès, and R. Liotta. Nuclear field theory. *Physics Reports*, 30:305, 1977.
37. D.R. Bès, G.G. Dussel, R.P.J. Perazzo, and H.M. Sofia. The renormalization of single-particle states in nuclear field theory. *Nuclear Physics A*, 293:350, 1977.
38. R. A. Broglia, P. F. Bortignon, F. Barranco, E. Vigezzi, A. Idini, and G. Potel. Unified description of structure and reactions: implementing the Nuclear Field Theory program. *Phys. Scr.*, 91:063012, 2016.
39. Bès, D. R. and J. Kurchan. *The treatment of Collective Coordinates in Many-Body Systems*. World Scientific, Singapore, 1990.
40. R. A. Broglia and A. Winther. *Heavy Ion Reactions*. Westview Press, Boulder, CO., 2004.
41. R. A. Broglia. Heavy ion reaction, notes of lectures delivered during the academic years 1974–1976 at SUNY, Stony Brook at Brookhaven National Laboratory, and at Niels Bohr Institute, unpublished. <http://www.mi.infn.it/~vigezzi/HIR/HeavyIonReactions.pdf>, 1975.
42. F. Barranco, G. Potel, R. A. Broglia, and E. Vigezzi. Structure and reactions of ^{11}Be : many-body basis for single-neutron halo. *Phys. Rev. Lett.*, 119:082501, 2017.
43. F. Barranco, G. Potel, E. Vigezzi, and R. A. Broglia. $d(^9\text{Li}, p)$, specific probe of ^{10}Li , paradigm of parity-inverted, soft-dipole isotones with one neutron outside the $N = 6$ closed shell. *Submitted to Phys. Rev. Lett.*
44. Barranco, F., P. F. Bortignon, R. A. Broglia, G. Colò, and E. Vigezzi. The halo of the exotic nucleus ^{11}Li : a single Cooper pair. *Europ. Phys. J. A*, 11:385, 2001.
45. Tanihata, I., M. Alcorta, D. Bandyopadhyay, R. Bieri, L. Buchmann, B. Davids, N. Galinski, D. Howell, W. Mills, S. Myhili, R. Openshaw, E. Padilla-Rodal, G. Ruprecht, G. Sheffer, A. C. Shotter, M. Trinczek, P. Walden, H. Savajols, T. Roger, W. Caamano, W. Mittig, P. Roussel-Chomaz, R. Kanungo, A. Gallant, M. Notani, G. Savard, and I. J. Thompson. Measurement of the two-halo neutron transfer reaction $^1\text{H}(^{11}\text{Li}, ^9\text{Li})^3\text{H}$ at 3A MeV. *Phys. Rev. Lett.*, 100:192502, 2008.
46. G. Potel, F. Barranco, E. Vigezzi, and R. A. Broglia. Evidence for phonon mediated pairing interaction in the halo of the nucleus ^{11}Li . *Phys. Rev. Lett.*, 105:172502, 2010.
47. Mahaux, C., P. F. Bortignon, R. A. Broglia, and C. H. Dasso. Dynamics of the shell model. *Physics Reports*, 120:1–274, 1985.
48. R.A. Broglia, G. Coló, G. Onida, and H.E. Roman. *Solid State Physics of Finite Systems: metal clusters, fullerenes, atomic wires*. Springer Verlag, Berlin, Heidelberg, 2004.
49. P. D. Nation, J. R. Johansson, M. P. Blencowe, and Franco Nori. Colloquium: Stimulating uncertainty: Amplifying the quantum vacuum with superconducting circuits. *Rev. Mod. Phys.*, 84:1, 2012.
50. R. M. Nugayev. Particle creation by a black hole as a consequence of the Casimir effect. *Communications in Mathematical Physics*, 111:579, Dec 1987.
51. I. Tanihata, H. Savajols, and R. Kanungo. Recent experimental progress in nuclear halo structure studies. *Progress in Particle and Nuclear Physics*, 68:215, 2013.
52. N. Keeley, N. Alamanos, and V. Lapoux. Comprehensive analysis method for (d, p) stripping reactions. *Phys. Rev. C*, 69:064604, 2004.
53. Tohru Motobayashi and Hiroyoshi Sakurai. Research with fast radioactive isotope beams at RIKEN. *Progress of Theoretical and Experimental Physics*, 2012, 2012.
54. Baroni, S., M. Armati, F. Barranco, R. A. Broglia, G. Colò, G. Gori, and E. Vigezzi. Correlation energy contribution to nuclear masses. *Journal of Physics G: Nuclear and Particle Physics*, 30:1353, 2004.
55. J.S. Winfield, S. Fortier, W.N. Catford, S. Pita, N.A. Orr, J. Van de Wiele, Y. Blumenfeld, R. Chapman, S.P.G. Chappell, N.M. Clarke, N. Curtis, M. Freer, S. Gals, H. Langevin-Joliot, H. Laurent, I. Lhenry, J.M. Maison, P. Roussel-Chomaz, M. Shawcross, K. Spohr, T. Suomijrvi, and A. de Vismes. Single-neutron transfer from $^{11}\text{Be}_{gs}$ via the (p, d) reaction with a radioactive beam. *Nuclear Physics A*, 683:48, 2001.
56. A. Pais. *Inward bound*. Oxford University Press, Oxford, 1986.
57. C. Bachelet et al. New Binding Energy for the Two-Neutron Halo of ^{11}Li . *Phys. Rev. Lett.*, 100:182501, 2008.
58. G. Potel, A. Idini, F. Barranco, E. Vigezzi, and R. A. Broglia. Nuclear Field Theory predictions for ^{11}Li and ^{12}Be : shedding light on the origin of pairing in nuclei. *Phys. At. Nucl.*, 77:941, 2014.
59. E. Schrödinger. Discussion of probability relations between separated systems. *Mathematical Proceedings of the Cambridge Philosophical Society*, 31:555, 1935.
60. P. W. Anderson. Special effects in superconductivity. In E. R. Caianello, editor, *The Many-Body Problem, Vol.2*, page 113. Academic Press, New York, 1964.
61. W.L. Mc Millan and J.M. Rowell. Tunneling and strong-coupling superconductivity. In R.D. Parks, editor, *Superconductivity*, volume 1, page 561, New York, 1969. Marcel Dekker, Inc.
62. M. Cavallaro, M. De Napoli, F. Cappuzzello, S. E. A. Orrigo, C. Agodi, M. Bondi, D. Carbone, A. Cunsolo, B. Davids, T. Davinson, A. Foti, N. Galinski, R. Kanungo, H. Lenske, C. Ruiz, and A. Sanetullaev. Investigation of the ^{10}Li shell inversion by neutron continuum transfer reaction. *Phys. Rev. Lett.*, 118:012701, 2017.
63. H. T. Fortune, G.-B. Liu, and D. E. Alburger. $(sd)^2$ states in ^{12}Be . *Phys. Rev. C*, 50:1355, 1994.
64. K. T. Schmitt, K. L. Jones, S. Ahn, D. W. Bardayan, A. Bey, J. C. Blackmon, S. M. Brown, K. Y. Chae, K. A. Chipps, J. A. Cizewski, K. I. Hahn, J. J. Kolata, R. L. Kozub, J. F. Liang, C. Matei, M. Matos, D. Matyas, B. Moazen, C. D. Nesaraja, F. M. Nunes, P. D. O'Malley, S. D. Pain, W. A. Peters, S. T. Pittman, A. Roberts, D. Shapira, J. F. Shriner, M. S. Smith, I. Spassova, D. W. Stracener, N. J. Upadhyay, A. N. Villano, and G. L. Wilson. Reactions of a ^{10}Be beam on proton and deuteron targets. *Phys. Rev. C*, 88:064612, 2013.
65. G. Bassani, N. M. Hintz, C. D. Kavaloski, J. R. Maxwell, and G. M. Reynolds. (p, t) Ground-State $L = 0$ Transitions in the Even Isotopes of Sn and Cd at 40 MeV, $N = 62$ to 64. *Phys. Rev.*, 139:B830, 1965.
66. Bechara, M. J. and O. Dietzsch. States in ^{121}Sn from the $^{120}\text{Sn}(d, p)^{121}\text{Sn}$ reaction at 17 MeV. *Phys. Rev. C*, 12:90, 1975.
67. F. Barranco, R. A. Broglia, G. Colò, G. Gori, E. Vigezzi, and P. F. Bortignon. Many-body effects in nuclear structure. *European Physical Journal A*, 21:57, 2004.
68. S. R. Lundeen and F. M. Pipkin. Measurement of the Lamb Shift in Hydrogen, $n = 2$. *Phys. Rev. Lett.*, 46:232, 1981.
69. A. Pais. *The genius of science*. Oxford University Press, Oxford, 2000.

- 70. Potel, G., A. Idini, F. Barranco, E. Vigezzi, and R. A. Broglia. Cooper pair transfer in nuclei. *Rep. Prog. Phys.*, 76:106301, 2013.
- 71. Bohr, A. and B. R. Mottelson. *Nuclear Structure, Vol.II*. Benjamin, New York, 1975.
- 72. B. R. Holstein. *Weak interaction in nuclei*. Princeton University Press, New Jersey, 1989.

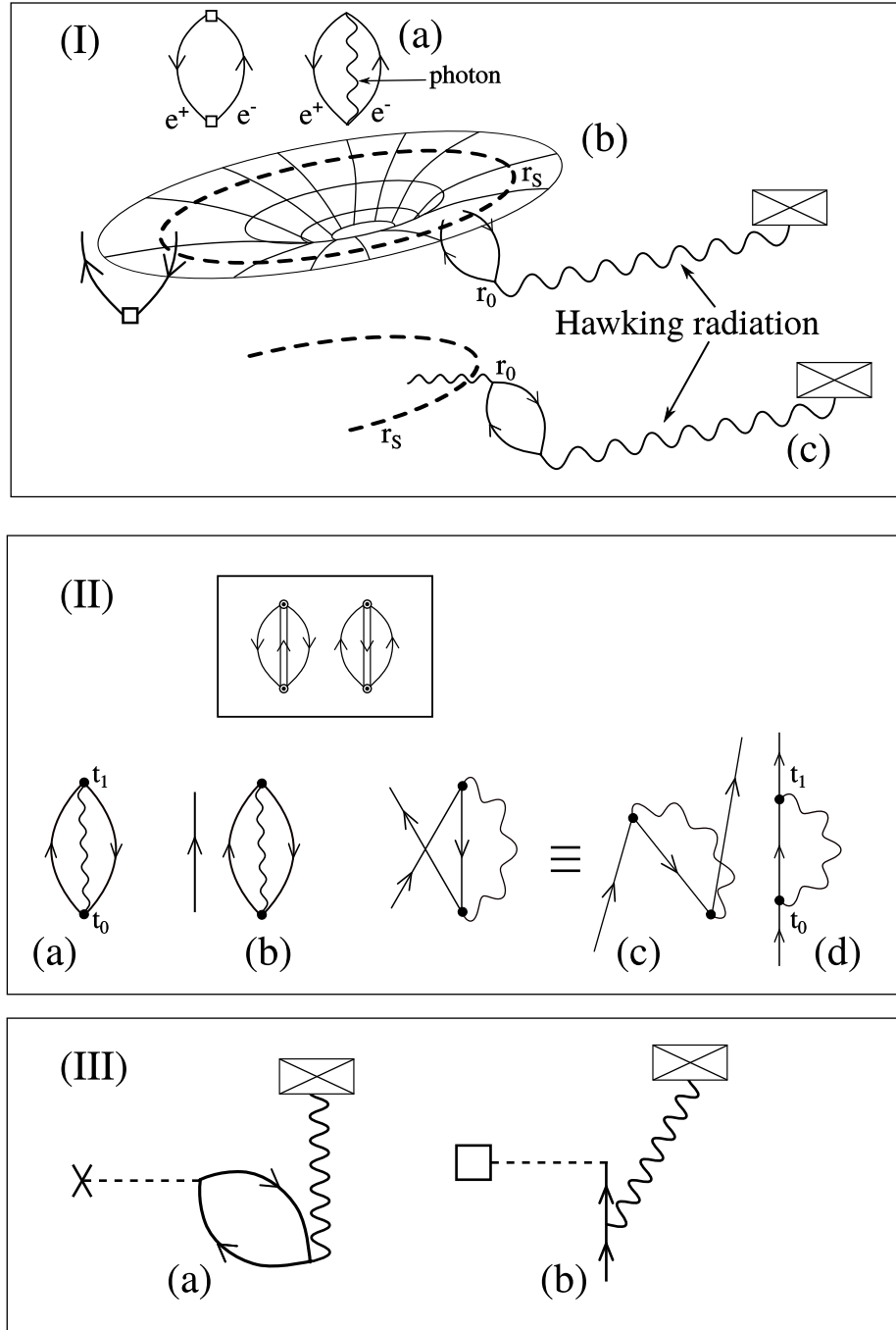


Fig. 1. (I) (a) ZPF of the QED vacuum produce virtual photons and electron-positron pairs. The virtual photon can be represented by the associated electromagnetic potential (empty square, left diagram, see also (b) left) or by a wavy line (right diagram) (see e.g. Figs. 8.11.1(a) and 8.11.2(b) of ref. [34]). When (b) the pair (c) or the photon) gets trapped behind the event horizon of a black hole, the point beyond which the gravitational pull is too strong even for light to escape, before the virtual process closes, the virtual photon (pair) become real. The photon (pair, eventually recombining in a photon) that escapes is emitted as Hawking radiation, which eventually can be recorded as a click in a detector (crossed rectangle). (II)(a) ZPF of the vacuum (ground) state of an even nuclear system (upward (downward) arrowed line representing a nucleon (nucleon hole); wavy line, a vibration); (b) odd system; (c) Pauli principle correction between the particle considered explicitly and those involved in the vibration (Lamb shift like diagram); (d) time ordering of the previous process. In the inset we show ZPF associated with addition and subtraction pairing vibrational modes (double arrowed lines). (III)(a) Acting with an external field (cross + dashed line, inelastic scattering e.g. (p,p')) on process (a) of (II) before it closes, that is at a time $t_0 < t < t_1$, one can force the virtual fluctuations of the vacuum to become real, and eventually observe a click in the detector (crossed rectangle). (b) Similar information is obtained by intervening process (d) of (II) with the appropriate external field (empty square + dashed line, e.g. (p,d) reaction).

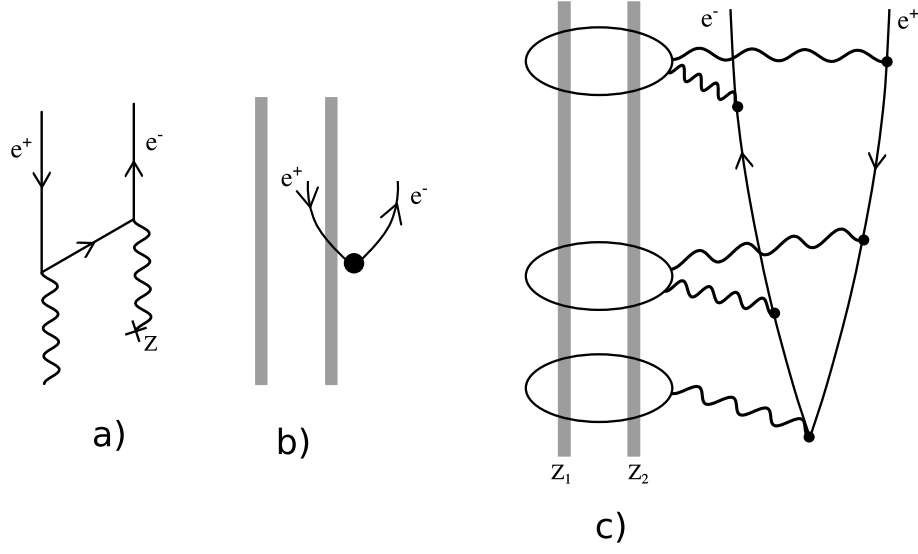


Fig. 2. Schematic representation of (a) Pair creation (arrowed lines pointing upwards (downwards) represent electrons (positrons), while wavy lines describe photons); (b) Hawking radiation, the hatched circle represents the left photon in (a) and the two vertices, the massive charge not being needed in presence of a black hole (Schwarzschild radius, hatched cylinder); (c) Transient quasimolecular state of two heavy ions at the distance of closest approach ($Z = Z_1 + Z_2 > Z_{crit} \approx 180$) making the QED vacuum unstable.

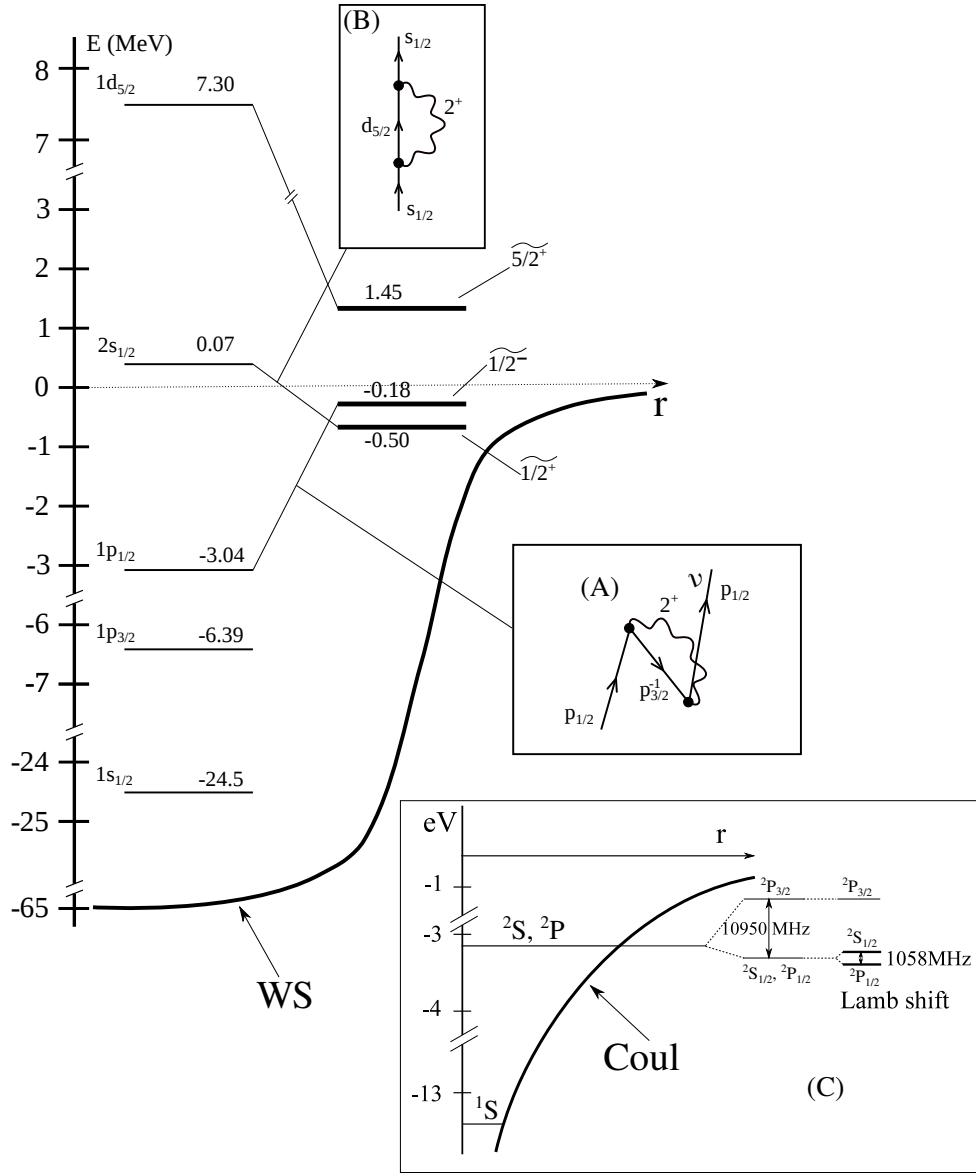


Fig. 3. Bare (thin) and dressed (bold face horizontal lines) single-particle levels of ^{11}Be calculated using a Woods-Saxon (WS) mean field. Due to the dressing of neutron motion with mainly quadrupole vibrations of the core ^{10}Be (insets (A) and (B)) inversion in sequence between the $2s_{1/2}$ and $1p_{1/2}$ levels (parity inversion) is observed. The numbers are energies in MeV. In inset (C), the lowest energy levels of hydrogen atom are indicated, the Coulomb potential (Coul) is also schematically shown. The effects of fine structure according to Dirac theory (l, s coupling plus relativistic mass increase) and Lamb shift associated with the splitting of the $^2S_{1/2}$ and $^2P_{1/2}$ levels are displayed.

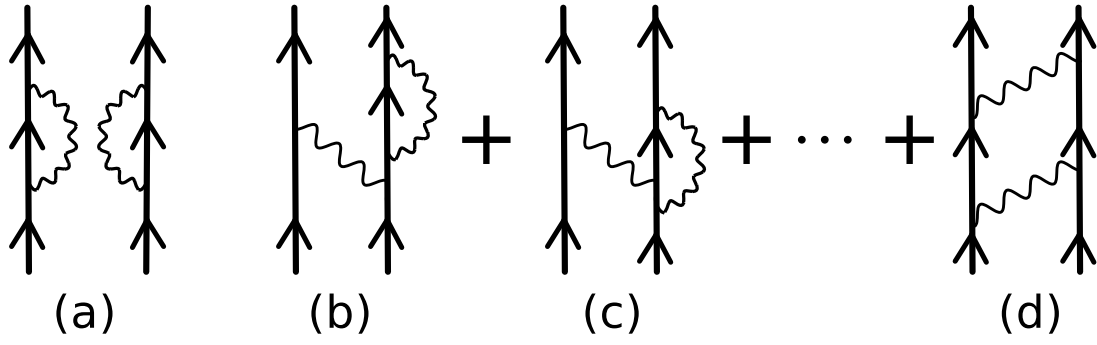


Fig. 4. (a) Self energy diagrams of two electrons (nucleons) e.g. of two hydrogen atom electrons (closed shell nuclei plus one nucleon), arrowed lines indicating the fermions, wavy-lines photons (nuclear particle-hole (ph) -like vibrations); (b) Coulomb interaction (induced nuclear interaction) resulting from the exchange of a photon ((ph)-vibration); (c) same as above but vertex corrected; (d) Van der Waals interaction (higher order induced nuclear interaction).

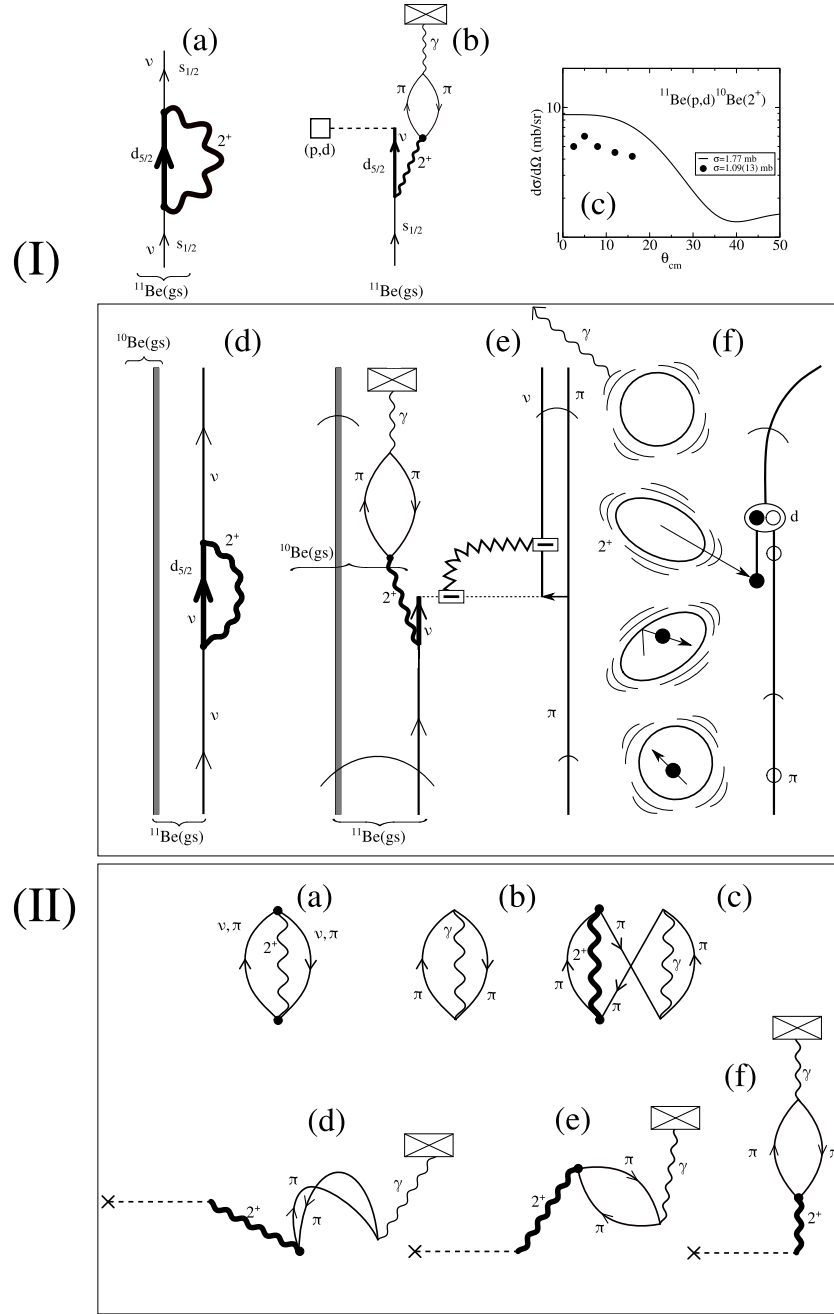


Fig. 5. (I) A virtual process in nuclear physics becomes real through the action of an external field. Arrowed lines pointing upwards (downwards) indicate a nucleon (p) (nucleon hole (h)) while wavy lines labeled 2^+ denote a quadrupole collective (ph) vibration. Bold face line stand for fully dressed modes (renormalization procedure [38]) (a) Clothing process of the $1/2^+$ parity inverted ground state of $^{11}_4\text{Be}_7$ through the coupling to the low-lying quadrupole vibration of the core $^{10}_4\text{Be}_6$; (b) schematic representation of the pickup of the neutron moving around a $N = 6$ closed shell and populating the low-lying quadrupole vibrational state of this core, in coincidence with the corresponding γ -decay (see also II (f)); the structure and reaction NFT diagram describing the pickup process in inverse kinematics, i.e. $^1\text{H}(^{11}\text{Be}, ^{10}\text{Be}(2^+, 3.368 \text{ MeV}))^2\text{He}$ is shown in (d) and (e) together with a cartoon representation in (f) (the jagged line represents a graphic mnemonic of the recoil effect, see [38] App. F as well as [70], App. A). Proton and neutrons are labeled π and ν respectively, while d stands for deuteron. Curved arrows indicate projectile motion (reaction). Normal arrowed lines, motion inside target or projectile (structure). (c) predicted (continuous curve) and experimental (solid dots) absolute differential cross sections associated with the indicated pickup process. (II) Interaction of protons in a nucleus with nuclear vibrations (solid dot, PVC vertex $\beta_L R_0 \partial U / \partial r Y_{LM}^*(\hat{r})$ [71], β_L : dynamical distortion parameter, $U(r)$ central potential) and photons (normal vertex, see also Fig. 1 (I)(a), electromagnetic interaction $e \int d^4x J_\mu(x) A^\mu(x)$, A^μ being the vector potential, and J_μ the current density ($\mu = 1, \dots, 4$) [72]). While the variety of diagrams shown have general validity, we have assumed we are dealing with the low-lying correlated particle-hole quadrupole vibration ($L = 2$) of $^{10}_4\text{Be}_6$ lying at 3.368 MeV, $B(E2; 0^+ \rightarrow 2^+) = 0.0052 e^2 b^2$ being associated with $\beta_2 \approx 0.9$. An arrowed line pointing upward (downward) describes a proton (proton hole) moving in the $p_{1/2}$ ($1p_{3/2}$) orbital. Zero point fluctuations of the nuclear ground state associated with: (a) the nuclear vibration, (b) the electromagnetic field associated with the corresponding spontaneous γ -decay. (c) Pauli principle correction to the simultaneous presence of the above two ZPF processes. (d) Intervening the virtual excitation of the nuclear vibrations (graph (c)) with an external (inelastic) field (cross followed by a dashed line), in coincidence with the γ -decay (γ -detector, crossed box), the virtual process (c) becomes real. (e), (f) time ordering of the above process correspond to the RPA contributions through backwardsgoing and forwardsgoing amplitudes [71] and subsequent γ -decay.

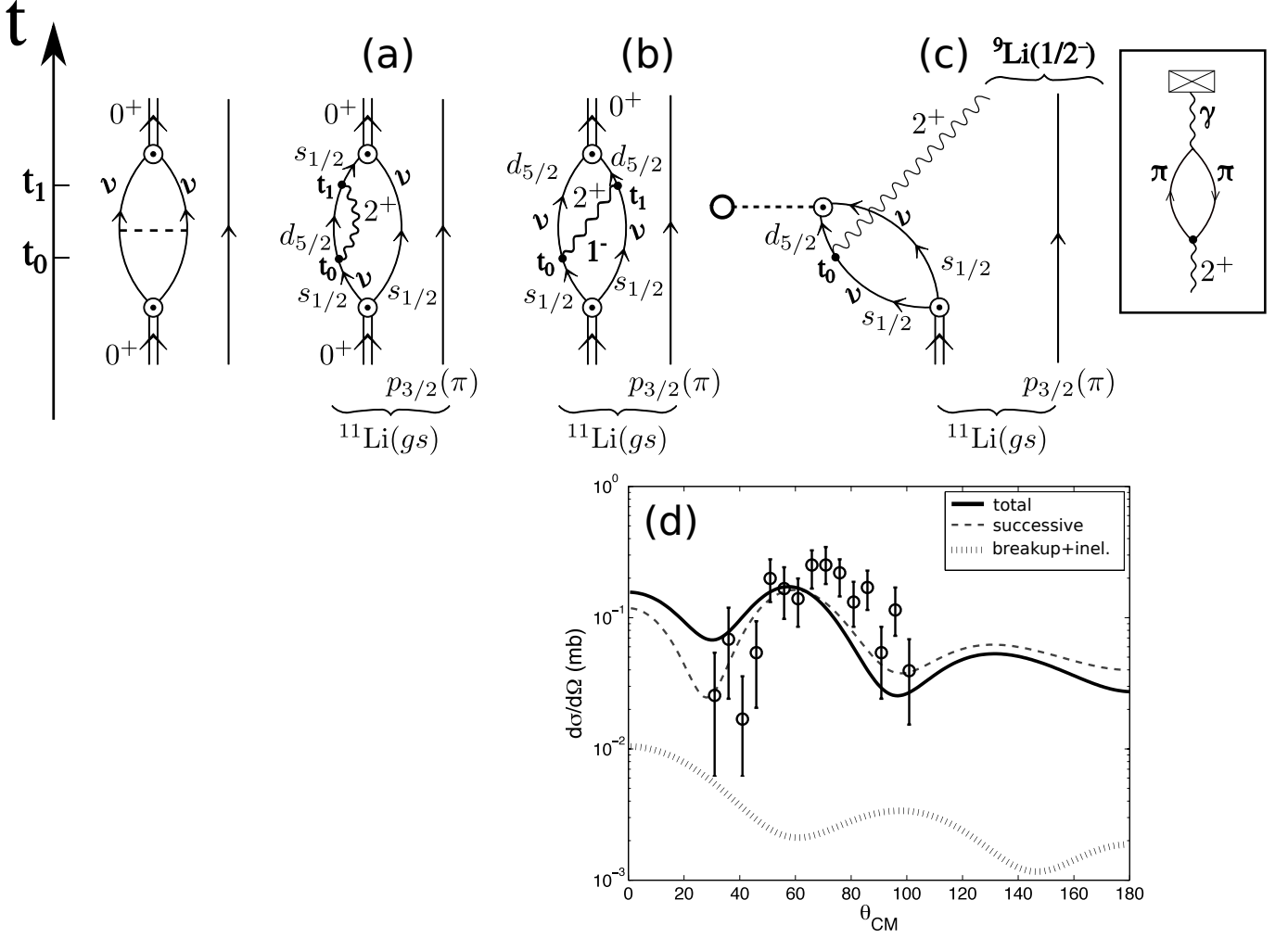


Fig. 6. (a),(b) Virtual process associated with the correlation of the two halo neutrons of $^{11}\text{Li}_8$ moving around the closed shell $N = 6$ core $^9\text{Li}_6$ due to the bare $NN^{-1}S_0$ interaction and to the exchange of collective vibrations, as well as the dressing of the halo neutrons. The odd $p_{3/2}$ proton (π) is assumed to act as a spectator; (c) an external two-neutron pickup field (open circle + dashed line) as provided by the inverse kinematic reaction $^1\text{H}(^{11}\text{Li}, ^9\text{Li}(1/2^-))^3\text{H}$ populates the lowest excited state of ^9Li , $1/2^-$ member of the multiplet ($p_{3/2}(\pi) \otimes 2^+$), forcing the 2^+ vibration of the core to become on shell and eventually by coupling to the electromagnetic field (see upper right boxed inset), γ -decay (HR) (further aspects of the physics associated with the reaction process are elaborated in connection with HR, see Fig. 5 (II)); (d): the theoretical absolute differential cross section (continuous curve) is compared with the data (open circles with error bars) in the lower box inset (see [45] and [46]).

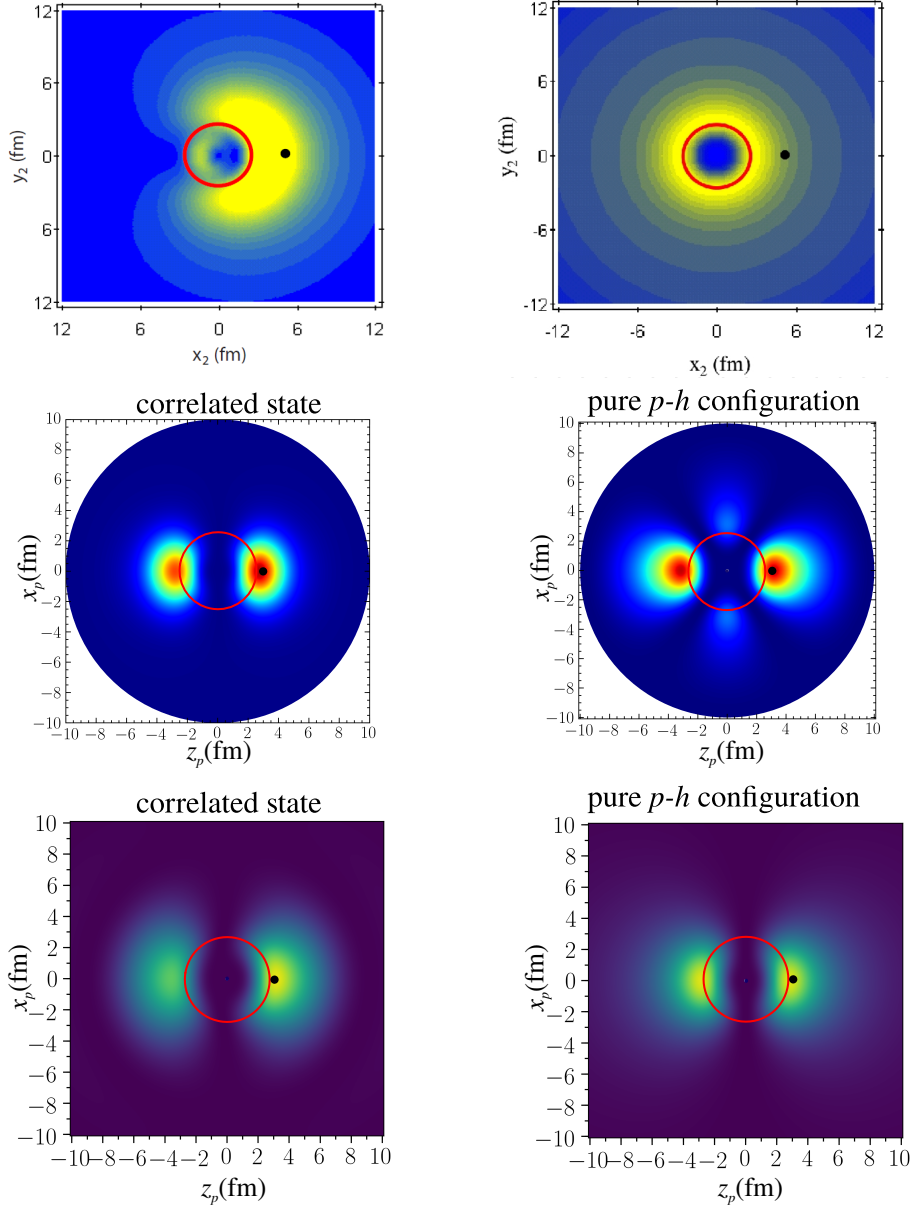


Fig. 7. (**Upper left**) Spatial structure of the neutron halo Cooper pair $|\tilde{0}\rangle_\nu$ entering in the ^{11}Li ground state $|\tilde{0}\rangle_\nu \otimes |p_{3/2}(\pi)\rangle$, the proton assumed to act as a spectator. The modulus squared of the wavefunction $\Psi_0(\mathbf{r}_1, \mathbf{r}_2) = \langle \mathbf{r}_1, \mathbf{r}_2 | \tilde{0} \rangle_\nu$ is displayed as a function of the Cartesian coordinates x_2, y_2 of particle 2, for a fixed position of particle 1 ($x_1 = 5$ fm, $y_1 = 0$; solid dot). The red circle represents the radius of ^9Li $R_0 = 2.5$ fm. (**Upper right**) same, but for the uncorrelated pure configuration $(p_{1/2})^2$. (**Middle left**) same as above, but for the $(p-h)$ quadrupole vibration of ^{10}Be . In this case the results are displayed in terms of the Cartesian coordinates (x_p, z_p) of the particle for a fixed position of the hole ($z_h = 3$ fm, $x_h = 0$ fm; solid dot). The red circle represents the radius of ^{10}Be $R_0 = 2.6$ fm. (**Middle right**) same, but for the neutron uncorrelated particle-hole configuration $((s_{1/2})^{-1}, d_{5/2})_{2+}$. (**Down left**) Same as above (middle) but for the case of the soft dipole mode of ^{11}Li . The radius is equal to that of the upper figure (**Down right**) same as above but for the uncorrelated neutron particle-hole configuration $((p_{1/2})^{-1}, s_{1/2})_{1-}$.

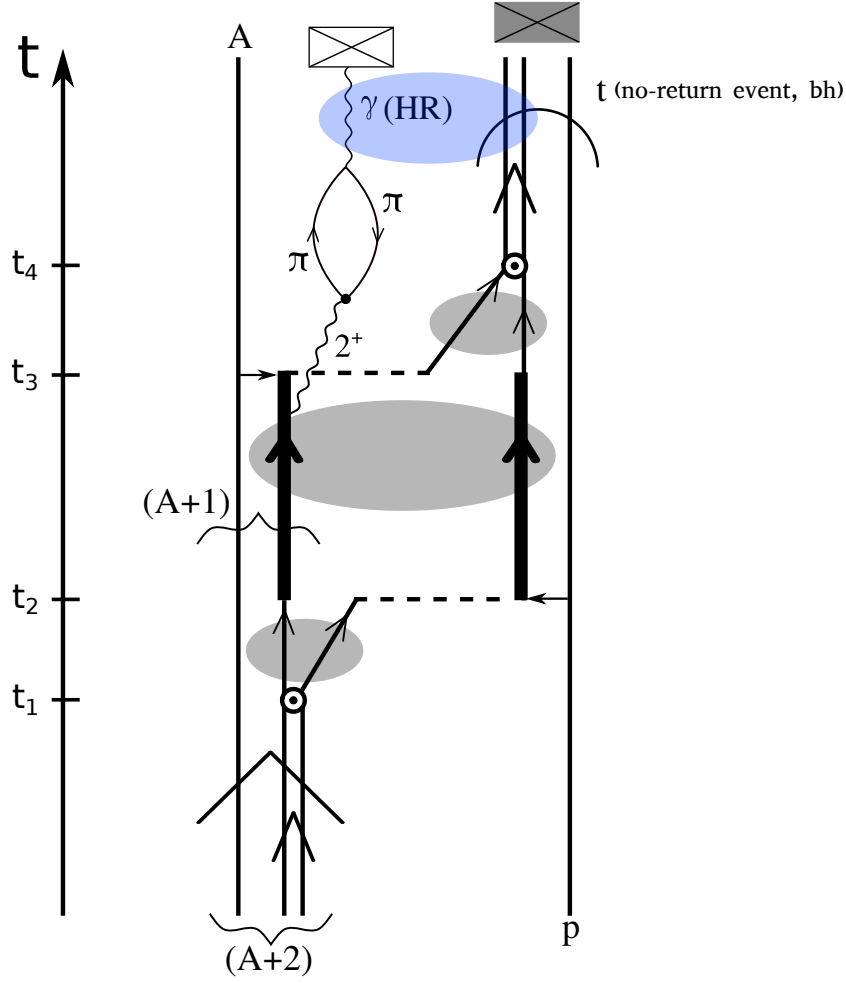


Fig. 8. General nuclear field theory diagram describing structure and reaction aspects of the main process through which a Cooper pair (di-neutron) tunnels from target to projectile in the reaction $(A+2) + p \rightarrow A + t$. In order that the two-step process $(A+2) + p \rightarrow (A+1) + d \rightarrow A + t$ takes place, target and projectile have to be in contact at least in the time interval running between t_2 and t_3 . During this time, the two systems create, with local regions of ever so low nucleonic presence, a common density over which the non-local pairing field can be established, and the Cooper pair can be correlated. Even with regions in which the pairing interaction may be zero. Small grey ellipses (with linear dimensions of the order of the nuclear radius R_0) indicate situations in which the two neutron correlation is distorted by the mean field of a single of the systems involved of the reaction, i.e. $A+2$ in the entrance channel, t in the exit one. Mean field which can be viewed as acting as an external field. The large grey ellipse (with linear dimensions of the order of ξ) indicate the region in which the two partners of the Cooper pair correlate over distances of the order of the correlation length. It is this information that the outgoing particle of a Cooper pair transfer process brings to the detector. In other words, this is the closest to what can be defined as the observable Cooper pair in terms of its specific probe, i.e. two-nucleon transfer process, and the reason why the neutrons are described, in the interval $\Delta t = t_3 - t_1$, in terms of bold face arrowed lines. In the present case the diagram is tailored to describe the process shown schematically in Fig. 6 (b), i. e. $^{11}\text{Li}(p, t)^9\text{Li}(1/2^-)$. Namely a situation in which the irreversible event associated with the tunneling of the second fermion takes place before the collective vibration is either reabsorbed by it, or is exchanged with the first neutron, forcing the collective mode to become on-shell and, after coupling to the electromagnetic field, escape the reaction area, entangled (large light blue ellipse) with the two fermions (neutrons) which have fallen into the no-return field of the triton (see Fig. 1 (I) (b)).

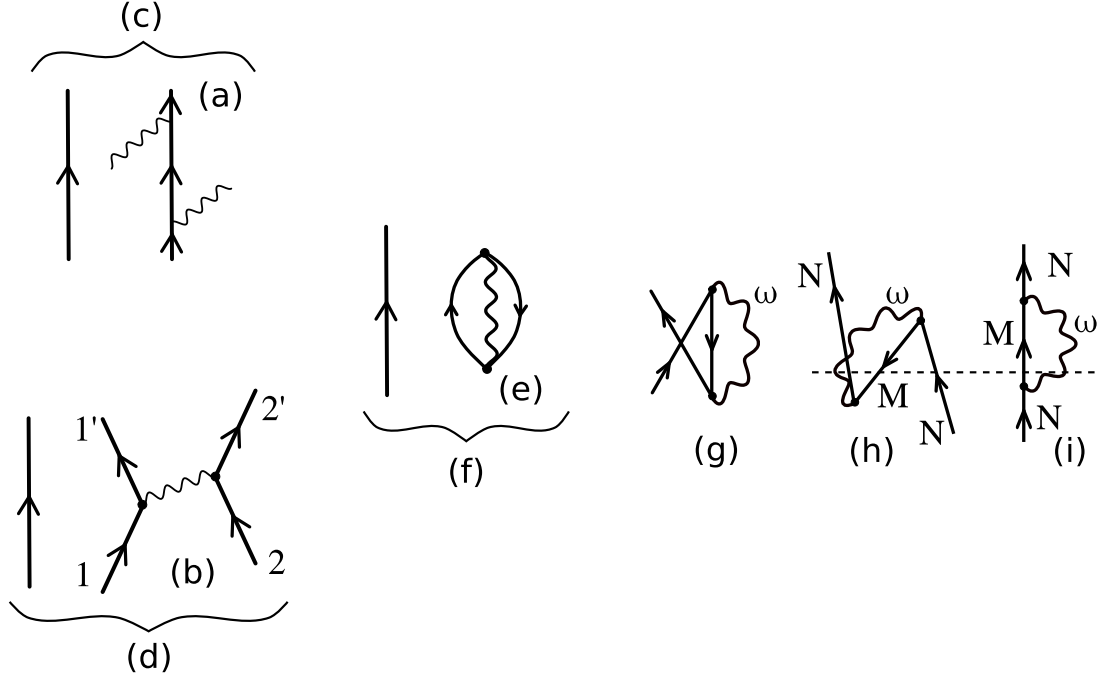


Fig. 9. (a) Lowest -order Feynman diagram for Compton scattering. (b) Scattering of two charged particles. Lines carrying arrows pointing upwards are electrons, downwards positrons, wavy lines being photons. At each vertex $V(t)$ (Eq. (11)) is operative. Time is assumed to run upwards. (c) and (d), same as (a) and (b) but with a disconnected electron line (spectator). (e) Joining two wavy lines, and the two electron lines of (a), or positron-electron lines (2 with 1, and 1' with 2') in (b) leads to the lowest-order, two vertex, vacuum fluctuation process. (f) Same as (e) but with the spectator electron line. (g) Process resulting from the exchange of the two electron lines. (h) Identical process to (g) redrawn to keep with standard presentation. (i) electron self-energy process resulting from the time ordering rearrangement of (h).